CLM - P 506

CLM - P 506

CULHAM LABORATORY
LIBRARY
23 JAN 1978
b
L

UKAEA

Preprint

THE XUV SPECTRA OF HIGHLY IONIZED MOLYBDENUM

M W D MANSFIELD
N J PEACOCK
C C SMITH
M G HOBBY
R D COWAN

CULHAM LABORATORY
Abingdon Oxfordshire

1977

This document is intended for publication in a journal or at a conference and is made available on the understanding that extracts or references will not be published prior to publication of the original, without the consent of the authors.

Enquiries about copyright and reproduction should be addressed to the Librarian, UKAEA, Culham Laboratory, Abingdon, Oxfordshire, England

CLM-P 506

THE XUV SPECTRA OF HIGHLY IONIZED MOLYBDENUM

M W D Mansfield*, N J Peacock, C C Smith*, M G Hobby

Culham Laboratory, Abingdon, Oxon OX14 3DB, U.K.
(Euratom/UKAEA Fusion Association)

and

R D Cowan

University of California Los Alamos Scientific Laboratory,
Los Alamos, New Mexico, U.S.A.

ABSTRACT

The spectra of molybdenum ions produced in Tokamaks in the wavelength range 10-200 Å have been reproduced in a plasma formed by laser beam irradiation of solid molybdenum targets. Lines from highly ionized stages of molybdenum (Mo XXX to Mo XXXII) have been distinguished by varying the laser beam intensity. Detailed analyses of the simpler ions, Mo XV (Ni-like), Mo XVI (Co-like), Mo XXXII (Na-like), and to a lesser extent Mo XXXI (Mg-like) and Mo XVII (Fe-like), have been achieved by comparison with ab initio calculations. A general interpretation of intermediate ion stages is also given but it is shown that most of these spectra are so complex, as a result of inner subshell excitation, that detailed term scheme analyses are nearly impossible.

(Submitted for publication in J. Phys. B, Atom. Molec. Phys.)

*Attached from Imperial College, London.

October 1977

1. INTRODUCTION

In recent years interest in the spectra of highly stripped molybdenum ions has grown considerably as a result of the frequent use of molybdenum metal for "aperture limiters" in Tokamak fusion devices e.g. ST Tokamak (Hinnov, Johnson, Meservey and Dimock 1972), TFR Tokamak (Equipe TFR 1975) and DITE Tokamak (DITE Tokamak Group 1977). Impurity ions of heavy elements such as molybdenum, and iron from the vacuum vessel walls, can make an important contribution to the effective charge state of the ions in the plasma. The electrical conductivity, spatial current distribution and power balance in the plasma column will thus be affected by the presence of impurities. At the electron temperatures existing in Tokamaks molybdenum is not fully stripped so that line radiation, particularly from low ionization potential molybdenum ions close to the limiter, is an important source of power loss from the plasma.

In order to determine quantities such as

$$Z_{eff} = \sum_{Z=1}^{Z_{max}} \frac{n_Z Z^2}{n_e}$$

and the radiative power loss, it is necessary to determine the spatial distribution, charge state and concentration of molybdenum impurities. The TFR group (Equipe TFR 1975), for example, have made fairly extensive measurements of these quantities based on a few $\Delta n = 0$ transitions in Mo XIV, Mo XXXI and Mo XXXII. A necessary first step in this process is, of course, to obtain unambiguous identifications of the lines emitted by molybdenum ions in Tokamaks. To date term scheme analyses of these spectra have been limited.

2. PREVIOUS MOLYBDENUM INVESTIGATIONS

The first review of the extreme ultraviolet spectra of molybdenum and adjacent elements in the periodic table was given by Édlen (1949) who identified the three Mo XVI transitions $3p^6 3d^9\ ^2D - 3p^5 3d^{10}\ ^2P$ in vacuum spark spectra. More recently Alexander, Even-Zohar, Fraenkel and Goldsmith (1971), studying a vacuum spark spectrum in the 45-350 Å wavelength range, have identified the $3d^{10} - 3d^9 4p$ transitions in Mo XV and $n = 4$ to $n = 5,6$ transitions in Mo XII, Mo XIII and Mo XIV. At longer wavelengths, 4s-4p transitions in Mo XIII and Mo XIV have been identified in the Princeton ST Tokamak (Hinnov et al. 1972) while more recently (Hinnov 1976) 3s-3p transitions in Mo XXXI and Mo XXXII have also been reported in the same device. In the X-ray region $2p^6 - 2p^5 3s$, $2p^5 3d$ transitions in Mo XXXIII have been seen in a laser produced plasma (Aglitskii, Boiko, Krokhin, Pikuz and Faenov 1975).

Theoretical calculations of energy levels of the molybdenum ions Mo XXIV, Mo XXX, Mo XXXI, Mo XXXII and Mo XXXIII have been performed by Klapisch, Perel and Weil (1976) using a relativistic, parametric potential method and, very recently, Schwob, Klapisch, Finkenthal and Schweitzer (1977) have identified some $\Delta n = 1$ Mo XXXII lines in the TFR Tokamak. Schwob et al. also make detailed assignments of $3p^6 - 3p^5 4d$ transitions in Mo XXV and 3d-4f transitions in Mo XXIV and give a general interpretation of molybdenum emission from lower degrees of ionization (Mo XV to Mo XXV). However, other than the fairly simple transitions summarized above, little detailed analysis of highly stripped molybdenum ions has been achieved.

In the present work the spectra from a laser produced molybdenum plasma have been photographed between 10 and 200 Å at various laser beam intensities at the target surface and these have been compared with spectra from the DITE Tokamak at the Culham Laboratory (DITE Tokamak group 1977). The electron density in DITE ($n_e \sim 10^{13}$ cm^{-3}) is very much lower than that in the laser produced plasma ($n_e \sim 10^{21}$ cm^{-3}). Collision rates are therefore very different in the two plasmas so that a comparison of the spectra enables identification of forbidden transitions from metastable levels to be made. Furthermore, spatial scans of the Tokamak emission show variations in the ion stage with location in the plasma, the ion stage in general increasing in charge state towards the core of the plasma.

3. EXPERIMENTAL DETAILS

Spectra were produced by irradiating a pure molybdenum target with a 30 GW 1.8 ns Nd laser (Peacock, Galanti, Jones and Lawson 1977). The degree of ionization in the plasma could be altered by varying the intensity of the laser beam, which was focussed via an aspheric F/1.4 Soro lens, from 5×10^{13} to 2×10^{14} W cm^{-2} at the solid target. The upper and lower intensity limits will be subsequently referred to as "high" and "low intensity". The spectra were photographed with a 5 m grazing-incidence GML5M spectrograph (Speer 1976) on Ilford Q2 plates. In using the GML5M spectrograph it was possible to vary the grazing angle continuously and to choose prefocussed grating modules according to the wavelength range under study. At short wavelengths (10 to 50 Å) a 600 ℓ mm^{-1} holographic grating was used at grazing angles of around 2°. At longer wavelengths (50 to 200 Å) a 316 ℓ mm^{-1} ruled grating at 3½° grazing angle was substituted. With a slit width of 3 microns, six shots were required on average to give adequate plate exposure.

Between 10 and 50 Å, wavelength calibration was achieved by the superposition of the Al XII resonance line at 7.756 Å and numerous Al XI lines between 30 and 50 Å. After applying corrections to account for discrepancies in molybdenum wavelengths

as measured in first and second order, the estimated wavelength uncertainty was $\pm$ 0.005 Å for lines from very highly stripped ions (Tables 1 and 2) and $\pm$ 0.01 Å for the less highly stripped ions of Tables 3 to 5. In the latter case, measurements depended largely on comparison with Alexander et al.'s (1971) molybdenum measurements and measurements of the same lines in the DITE Tokamak spectrum. In the wavelength range 50 to 200 Å, the calculated instrumental dispersion was fitted to the Mo XV lines at 50 Å and their second order values. The wavelength accuracy is estimated to be $\pm$ 0.02 Å from an examination of several lines between 60 and 90 Å and their second order values.

DITE spectra in the range 10 to 300 Å were photographed on SC5 plates with a 2m Hilger and Watts E580 spectrograph which was fitted with a 1200 ℓ mm^{-1} ruled grating, used at 2° grazing angle. The molybdenum spectrum in the Tokamak (figure 1) is overlaid with many other impurity lines notably of oxygen, nitrogen, carbon, iron, chromium and nickel. The central 125 msec of each 250 msec pulse was selected by mechanical shuttering, and plate exposures varied from ten shots at 50 kA heating current to five shots at 200 kA. Radial scans of the DITE plasma proved useful in separating spectra from different ion stages.

4. RESULTS

4.1 Experimental

The molybdenum spectrum between 10 and 100 Å, as observed in the DITE Tokamak, is reproduced in figure 1 where it is compared with emission from a laser-irradiated target at "low" beam intensity. In both these spectra the plasma temperature is relatively low (T_e < 500 eV). In these conditions the molybdenum spectrum below 30 Å comprises only broad bands of emission resulting from $\Delta n = 1$ transitions in lower degrees of ionization (approximately up to Mo XXIV), figure 1, so that the strong discrete line spectrum which appears in the "high" density laser-produced spectrum, figure 2, is entirely attributable to higher ionization stages. These lines have not yet been observed in the DITE Tokamak although some have been reported in the TFR Tokamak (Schwob et al. 1977) where higher temperatures ($T_e \sim$ 1.5 keV) have been attained. At longer wavelengths there are also many lines which are peculiar to the high intensity plates. These are shown, figure 3, in a comparison of high and low intensity plates in the wavelength range 50 to 140 Å.

All lines clearly attributable to high ion stages are listed in tables 1 and 2 and lines from lower stages of ionization are listed in tables 3 to 5. Note that for the lower degrees of ionization we have only listed lines for which clear identifications are possible. As may be seen from figure 1, there are a considerable number of lines from lower ionization stages whose wavelengths we have not given here, notably the strong dense band of lines extending from 65 to about 90 Å.

4.2 Theoretical

Two different ab initio Hartree-Fock programs were used to interpret the spectrum. The general assignments for lower ion stages shown in figure 1 and the energy calculations presented in figures 4, 5 and 10 were made using the program MCHF72 (Froese-Fischer 1972). This program is non-relativistic and was usually operated in the single configuration approximation, so that the results are not considered sufficiently accurate to justify detailed comparisons with observations.

For detailed comparison with observation (Tables 1 to 5) and for oscillator strength calculations (figure 9) the HXR method (Cowan and Griffin 1976) has been used. This program incorporates the main relativistic effects in the radial wavefunctions and is thus more suitable than the Froese code for the heavy ions we are concerned with here.

5. DISCUSSION

5.1 MoXXXII (Na-like)

On comparing high intensity spectra with the present ab initio calculations and with the calculations of Klapisch et al. (1976) definite identifications can be made for the Na-like ion Mo XXXII, as shown in table 1. The lines at 126.94 and 127.81 Å are of special interest as they are probably the origin of the line at 129 $\pm$ 0.5 Å (Hinnov 1976) which has been used extensively in molybdenum concentration estimates (Equipe TFR 1975). The 129 Å line in the TFR Tokamak was treated as purely Mo XXXII 3s-3p for diagnostic purposes. The present wor indicates that it should really be considered to be a blend of two Mo XXXII transitions, $3p_{5/2} - 3d_{5/2}$ at 126.94 Å and $3s_{\frac{1}{2}} - 3p_{3/2}$ at 127.81 Å. Our identifications are in reverse order to the predictions of Klapisch et al. (1976). The present identifications are more satisfactory as they lead to a ζ_{3p} value which is in good agreement with that obtained from other observed 3p-nl lines and with the calculated values, whereas the order suggested by Klapisch et al. produces a ζ_{3p} greater than the other observed values by considerably more than the estimated errors.

5.2 Mo XXXI (Mg-like) and Mo XXX (Al-like)

All other lines from plasmas produced by high intensity beams are listed in table 2 where they are compared with the calculations of Klapisch et al. (1976) as well as with the present calculations. Correlation between observation and calculations is generally good for the Mo XXXI (Mg-like) n = 3 to n = 4 transitions which occur between 10 and 19 Å (table 2.1) so that detailed assignments should be correct. The theoretical accuracy is much poorer for the n = 3, Δn = 0, transitions which are listed in table 2.2, however, so that

detailed assignments are justified for only the five strongest lines.

The line which has been observed at 117 $\pm$ 0.5 Å (Hinnov 1976) in the TFR Tokamak (Equipe TFR 1975) is probably the strong line measured to lie at 115.97 Å in the present investigation (Table 2). The TFR identification of the line as Mo XXXI $3s^2\ {}^1S_0 - 3s3p\ {}^1P_1$ is almost certainly correct.

It will be noted that few Mo XXX (Al-like) assignments are proposed in Table 2. This is largely because wherever a Mo XXXI assignment is possible it has been used, leaving very little structure to be accounted for as Mo XXX, especially at short wavelengths. The Mo XXX spectrum is probably present at a much greater strength than is indicated by the assignments of table 2. Many of the excited configurations contain three open subshells so that a very complex spectrum is expected. Mo XXX may therefore be expected to manifest itself in broad bands of emission, making detailed identification difficult.

5.3 Inner subshell excitation

Before proceeding to a detailed analysis of lower ionization stages of molybdenum it is pertinent to consider the general importance of inner subshell transitions in highly stripped ions of heavy elements.

In a very highly stripped ion, the central field is very strong and hence there is a tendency towards ℓ-degeneracy in the energy level structure. This occurs not only in the energies of levels produced by excitation of a valence electron but also in the energy required to excite an electron from an inner subshell.

Let us consider, as an example, the effect of the trend towards inner subshell ℓ-degeneracy on the spectrum of the K-like ion Mo XXIV. In Figure 4 the energy levels of this ion are compared with those of neutral potassium. When one considers only excitation of the valence subshell in Mo XXIV (second column of figure 4), the energy level diagram shows the expected trend towards ℓ-degeneracy, although it is no more complex than the simple alkali diagram of K I (first column of figure 4). However when inner subshell excitation in Mo XXIV is included (third column of figure 4) the diagram changes fundamentally. The lowest odd configuration becomes $3p^5 3d^2$ and the lowest excited even configuration is $3s3p^6 3d^2$. Each configuration $3p^6$ nl is accompanied at slightly higher energies by similar configurations in which one

or more 3s or 3p subshell electrons have entered 3d orbitals e.g. $3p^5 3d\ nl$, $3s3p^6 3d\ nl$, $3p^4 3d^2\ nl$ etc. Energies are determined mainly by the values of the principal quantum numbers.

Notable consequences of inner subshell excitation are as follows:-

1) The energy level structure is vastly more complex than that of K I. For simplicity only a few configurations resulting from inner subshell excitation are shown in figure 1 and for these only configuration spreads are indicated. The configuration $3p^5 3d^2$ for example produces 43 levels with J values ranging from $\frac{1}{2}$ to $^{11}/_2$.

2) The resonance transitions of Mo XXIV are $3p^6 3d - 3p^5 3d^2$. The energy needed to excite these transitions, approximately 125 eV, is much less than the energy required to excite $3p^6 3d - 3p^6 4p$ or $3p^6 4f$ transitions (477 and 571 eV respectively).

3) There is also a tendency towards ℓ-degeneracy in the Mo XXIV ionization thresholds, levels of Mo XXV. Configurations such as $3p^5 3d$ and $3s3p^6 3d$ lie just above the first ionization limit, $3p^6$. The Mo XXIV ionization potential is thus much less clearly defined than in a simple alkali. There will be considerable overlap of high series members converging on Mo XXIV ionization thresho and there is therefore little prospect of observing extended Rydberg series.

4) The complex configurations resulting from 3p-or 3s-subshell excitation possess a large range of J-values. In consequence there are many levels of high statistical weight just above the ground state and many of these levels are metastable.

5) The excited configurations resulting from 3p-or 3s-subshell excitation to 3d orbitals belong to the same configuration-mixing complexes and configuration-mixing effects should be important. The configurations $3p^6 3d$, $3s3p^6 3d^2$ and $3p^4 3d^3$ shown in Figure 4 are examples of configurations which should mix strongly.

Although so far we have restricted discussion to the K-like ion Mo XXIV it is clear that similar effects are to be expected in any highly stripped ion in which there are inner subshells of the same principal quantum number as the valence electrons. In the n = 2 row of iso-electronic sequences (B-like to F-like) excitation of the 2s-subshell is a fairly simple example of this effect and is generally taken into account in the analysis of spectra from these ions. In the present study of molybdenum we are concerned with the n = 3 row (Al-like to Co-like). Excitation of one or more of the eight inner electrons in the 3s- and 3p-subshells must now be considered. We have seen how the spectrum of a simple ion such as Mo XXIV became much more complex. For other ions in the n = 3 row, which are

mostly iso-electronic with transition elements, already complex spectra become vastly more complex.

The trend towards ℓ-degeneracy in highly stripped ions also has a marked effect on the variation of ionization potential with degree of ionization and hence on the distribution of the various stages of ionization in a plasma. In figure 5 the ionization potentials of Mo ions ranging from Mo X (As-like) to Mo XXXIII (Ne-like), as computed from configuration average Hartree-Fock calculations, are shown. The variation is generally smooth. Large steps occur only when a new shell is broken into at n = 3 (Mo XV, Ni-like) and n = 2 (Mo XXXIII, Ne-like). At new subshells, such as the 3p-subshell at Mo XXV, (Ar-like) there are only small steps in the curve.

5.4 MoXIII (Zn-like) to Mo XXIX (Si-like)

At low laser beam intensities (figure 1) the lines assigned to Mo XXXI and Mo XXXII disappear from the Mo spectrum. Emission in the 10 to 200 Å range may then be divided into two distinct regions:-

1) The region above 60 Å where a very dense band of emission lines extends from 65 Å to longer wavelengths. The band steadily weakens above 80 Å.

2) The region between 60 and 15 Å where regular bands of emission, each about 2 Å broad, are observed. The longer wavelength bands between 55 and 40 Å comprise well-spaced groups of resolvable emission lines. Towards shorter wavelengths the lines tend to merge into diffuse bands of emission until, at about 22 Å, the bands themselves merge to produce a region of almost continuous emission. Below 18 Å weak band structure is again evident down to 15 Å where the spectrum finally dies out.

5.4.1 65-100 Å $\Delta n = 0$ transitions

By means of comparison with Hartree-Fock calculations the broad band of emission which starts above 65 Å may be clearly identified with $3p^6 3d^n - 3p^5 3d^{n+1}$ transitions in Mo XVI and higher degrees of ionization. An interesting feature of these transitions is that they move to longer wavelengths as the degree of ionization increases. This effect, illustrated in figure 5, arises directly from the trend towards ℓ-degeneracy with increasing ionic charge. The shortest wavelength lines thus come from the lowest degrees of ionization and the band cuts off abruptly below 65 Å because, for ions less highly ionized than Mo XVI, the 3d-subshell is full in the ground state and 3p - 3d excitation is no longer possible. $3p^5 3d^{n+1}$ levels are greatly spread out due to the large values of the (3p3d) electrostatic interaction and the spin-orbit interaction ζ_{3p}. This leads to considerable overlap between 3p - 3d lines in different stages of ionization as indicated in figure 1. This overlap, together with the rather poor

accuracy of ab inito calculation of $\Delta n = 0$ transitions, means that it is difficult to achieve an unambiguous interpretation of the low intensity spectrum above 65 Å. Detailed ab initio calculations have been performed for 3p - 3d transitions in Mo XVI and Mo XVII. The three lines expected in Mo XVI, $3p^6 3d^9\ ^2D - 3p^5 3d^{10}\ ^2P$, have already been identified by Edlén (1947). In table 4 their energies are compared with ab initio estimates. Calculated energies are about 2% too low but observed intensities agree quite well with the calculated gf values. For the more complex case of Mo XVII $3d^8 - 3p^5 3d^9$ some agreement was found between observation and calculation but, until the influence of 3p - 3d transitions in Mo XVIII and higher degrees of ionization in this wavelength region is understood in detail, assignments are considered to be too uncertain to justify a detailed listing. It will probably be necessary to study these transitions in adjacent isoelectronic ions before assignments can be made with confidence. Note too that some of the stronger 3s - 3p transitions in Mo XXVI to XXIX will also lie in this energy region.

5.4.2 15-60 Å $\Delta n > 0$ transitions

In the second region, between 60 and 15 Å, the low power Mo spectrum comprises mainly well spaced bands of emission. These are broadly identified (figure 1) as $\Delta n = 1$ (3d - 4p, 3d - 4f, 3p - 4s, 3p - 4d and 3s - 4p) transitions in Mo XIII to Mo XXIV and probably higher stages of ionization. In each ion the lowest energy $\Delta n = 1$ transitions are 3d - 4p. As shown in figure 5, 3d - 4p energies increase with the degree of ionization unlike the 3p - 3d transitions discussed above. The simplest 3d - 4p transitions are $3d^{10}\ ^1S_o - 3d^9 4p$ (J = 1) in Mo XV. These lines have been identified by Alexander, Even-Zohar, Fraenkel and Goldsmith (1971) and are compared with the present calculations in Table 3. The calculated energies for these $\Delta n = 1$ transitions agree with observation to within 0.2%, which is notably better than the 2% agreement obtained for $\Delta n = 0$ transitions in Mo XVI. The observed intensity ratio for the 50.435 and 49.899 Å lines is 5:4, rather different from the calculated oscillator strength ratio of about 4:1 which implies that these levels are not populated by ground state excitation alone. Alexander et al.'s (1971) third $3d^{10} - 3d^9 4p$ line at 50.920 Å was not observed in the present investigation. The calculated oscillator strength of this transition ($^1S_o - {}^3P_1$) is only 1/750 of the calculated strength of the 50.435 Å ($^1S_o - {}^1P_1$) line. Proceeding to shorter wavelengths in figure 1 it is clear that at least the next five bands may be identified with 3d - 4p excitation in increasing ionization stages, from Mo XVI to Mo XX. For Mo XVI $3d^9 - 3d^8 4p$ and Mo XVII $3d^8 - 3d^7 4p$ transitions detailed comparisons have been made between observed and calculated energies and intensities. The agreement,

illustrated in Table 4 and figure 6 for Mo XVI, and Table 5 and figure 7 for Mo XVII, is sufficiently good to justify the detailed assignments listed in these tables. It should be noted that the calculations confirm that for these bands of lines there is very little overlap between the different ionization stages so that each band may be associated with a single stage of ionization, in marked contrast to the situation noted earlier for 3p - 3d excitation in these ions.

We also expect to see 3d - 4p excitation in Mo XIII and Mo XIV as the $3d^9 4s^2 4p$ and $3d^9 4s4p$ levels lie below the first ionization potentials of their respective species, as shown in figure 5. Lines are observed in the expected wavelength region (50 to 55 Å) of the laser produced plasma spectrum but comparisons between calculation and observation are not as satisfactory as they were for Mo XV, XVI and XVII so that assignments are not considered sufficiently reliable to justify a detailed listing. For the Mo XIV configuration, $3d^9 4s4p$, the presence of a single 4s electron introduces new possibilities of configuration mixing. Inclusion of $3d^9 4p4d$ mixing with $3d^9 4s4p$ considerably improves agreement between observation and calculation. Assignment of $3d^{10} 4s - 3d^9 4s4p$ lines in Mo XIV is also made more difficult by the large (4s4p) electrostatic interaction which spreads the upper levels and leads to some overlap with 3d - 4p transitions in Mo XV and Mo XIII.

Towards shorter wavelengths in figure 1 it becomes more difficult to resolve discrete line structure in the bands, which appear as diffuse bands of emission. It is easy to understand how this happens in general terms. As the 3d-subshell empties the lower and upper configurations, $3d^n$ and $3d^{n-1} 4p$, produce vastly more complex level structures. Each ion produces hundreds of lines which merge into irresolvable bands of emission. However as the 3d-subshell becomes almost empty we should expect the spectrum to simplify. In Mo XXIV (K-like) we should see only 3 lines, $3d\ ^2D - 4p\ ^2P$, at about 26 Å. Figure 1 however shows only broad bands in the region where these lines are expected.

The breadths of the shorter wavelength bands and their persistence to 15 Å may be understood in terms of <u>other</u> $\Delta n = 1$ transitions, namely the 3d - 4f transitions and the inner subshell transitions 3p - 4s, 3p - 4d and 3s - 4p. The average wavelengths of these bands of transitions are indicated in figure 1 and it is clear that below 36 Å there will be substantial overlap between the 3d - 4p bands and other $\Delta n = 1$ bands.

In Mo XV and Mo XVI it is possible to separate the 3d - 4f transitions from underlying 3d - 4p bands in higher degrees of ionization. The Mo XV $3d^{10}\ ^1S_o - 3d^9 4f\ ^1P_1$ line, reported in the TFR Tokamak (Schwob, Klapisch, Finkenthal and Schweitzer 1977), is clearly observed at 35.363 Å (Table 1). A weaker line at 36.198 Å is assigned $3d^{10}\ ^1S_o - 3d^9 4f\ ^3D_1$. However as the $^1S_o - ^3D_1$ transition is estimated to possess only 4% of the $^1S_o - ^1P_1$ strength

and as the lines lies in the Mo XIX $3d^6$ - $3d^5 4p$ band, the assignment is uncertain. For Mo XVI $3d^9$ - $3d^8 4f$ good agreement between observation and calculation is obtained for the stronger lines (Table 4 and figure 8). Many weaker $3d^9$ - $3d^8 4f$ are also expected between 33 and 34 Å, and indeed are probably present in figure 8. However these weaker lines overlap the Mo XX $3d^5$ - $3d^4 4p$ band and, as it has not yet been possible to separate the two groups of lines, they are not listed in table 4.

Thus it is clear that from 33 Å downwards each band will result from the superposition of $\Delta n = 1$ transitions in different stages of ionization. Eventually, at 20 Å (figure 1), the bands superpose less exactly and one broad region of emission results. The relative strengths of the various $\Delta n = 1$ transitions have been estimated by oscillator strength calculations for Mo XV to XXVI (Figure 9), Oscillator strengths in the ions Mo XV, XVI, XXIV and XXVI have been calculated in detail. In other ions they are determined by interpolation. Figure 9 shows that 3d - 4f transitions are by far the most probable in Mo XV but that they weaken steadily with increasing degree of ionization. 3p - 4d transitions on the other hand strengthen with increasing degree of ionization until by Mo XXV they should be the strongest.

There are however clear differences between these calculated $\bar{f}$-values and observed intensities in Mo XV and XVI. From calculation 3d - 4f should be ten times stronger than 3d - 4p, whereas the observed lines of these two sets of transitions are of similar strength. It seems clear therefore that $3d^{n-1}4p$ levels are populated by downward cascading of the type $3d^{n-1}4f \rightarrow 3d^{n-1}4d \rightarrow 3d^{n-1}4p$ as well as by ground state excitation. This effect is illustrated in figure 10, the energy level diagram of Mo XV. Note that the cascade can end on the $3d^9 4s$ metastable levels which can also be fed by the $3p^5 3d^{10}$ nl cascade.

It is reasonably straightforward therefore to explain how the $\Delta n = 1$ bands of Mo persist down to 15 Å and why they tend to merge below 22 Å by including the effects of inner subshell excitation from the 3s- and 3p-subshells. The return of weak band structure below 18 Å probably occurs as 3d-4p and 3d-4f transitions weaken (figure 9), leaving mainly 3p - 4d band structure, although it is clear from the preceding analysis of Mo XXXII (5.4.1) that 3d - 4f transitions persist long after the lower configuration is no longer the ground configuration.

We have still to explain the absence of discrete Mo structure below 28 Å in figure 1. Figure 9 leads us to expect strong and simple transitions in Mo XXIV, $3d\ ^2D - 4f\ ^2F$ and Mo XXV, $3p^6\ ^1S_o - 3p^5 4d$ (J = 1). They will be overlapped by 3p - 4d, 3s - 4p and possibly $\Delta n = 2$ bands in lower degrees of ionization but should nonetheless appear as sharp lines superposed on the bands. In order to understand the absence of simple structures we should recall the discussion of inner subshell excitation (section 5.3) where it was noted that inner subshell transitions produce excited configurations of high statistical weight just above the ground state. For Mo XVI to XXV the most important of these configurations is $3p^5 3d^{m+1}$. The influence of this configuration grows rapidly as the 3d-subshell empties, an effect which is illustrated in figure 11 by plotting the ratio of the total statistical weight of $3p^{n-1}3d^{m+1}$ levels to the total statistical weight of the levels of the ground configurations $3p^n 3d^m$. As shown in figure 5, $3p^{n-1}3d^{m+1}$ configurations lie only about 120 eV above the ground state in the Mo ions we are considering so that in the laser produced plasma a statistical distribution of population between the ground levels $3p^n 3d^m$ and $3p^{n-1}3d^{m+1}$ levels may be expected. This leads to substantial non-ground state populations for Mo ions from Mo XX to Mo XXVIII. The situation is most acute in Mo XXIV (K-like) and Mo XXV (Ar-like), the very ions in which we might anticipate a few strong transitions to the ground state. With most of the population in $3p^5 3d^2$ and $3p^5 3d$ levels we now expect to see $3p^5 3d^2 - 3p^5 3d4f$ transitions in Mo XXIV and $3p^5 3d - 3p^4 3d4d$ transitions in Mo XXV. Examination of figure 4 shows that energy separation of the $3p^5 3d^2$ and $3p^5 3d4f$ configurations in Mo XXIV is essentially the same as the 3d-4f separation. Similarly $3p^6 - 3p^5 4d$ and $3p^5 3d - 3p^4 3d4d$ in Mo XXV have the same energy separation. This means that in both cases, and in fact in all cases in these ions, the simple transitions will be lost in a band of stronger complex non-ground state transitions. There is therefore some doubt about the Mo XXIV and Mo XXV identifications proposed in the TFR tokamak spectrum (Schwob et al. 1977).

In Tokamaks $3p^{n-1}3d^{m+1}$ levels derive additional interest because, from Mo XXI to Mo XXVIII, many are metastable and may thus be expected to attain substantial populations. The occurrence of metastable levels will tend to invalidate the use of a coronal model and, furthermore, it may be possible to observe forbidden transitions from these levels to the ground states.

Note that for simplicity only the statistical weight ratios between $3p^{n-1}3d^{m+1}$ configurations and $3p^n 3d^m$ ground configurations have been considered in figure 11. Other low lying excited configurations such as $3p^{n-2}3d^{m+2}$, $3s3p^n 3d^{n+1}$ and $3s3p^{n+1}$ (in Mo XXVI and higher degrees of ionization) will also compete for population.

5.4.3 Forbidden transitions

As noted in section 2 electron densities, and hence collision rates, in Tokamak plasmas are very much lower than in laser produced plasmas. In a laser produced plasma metastable levels, such as the Mo XV $3d^9 4s$ levels shown in figure 10, are collisionally depopulated before they can radiate and therefore transitions from these levels are not observed. In contrast it may be deduced that, in the outer regions of a tokamak plasma, the probability of collisional depopulation of the $3d^9 4s$ (J = 2) levels is about two orders of magnitude less than the probability of their decay to the ground state by electric quadrupole radiation. Forbidden Mo XV $3d^{10}\ {}^1S_0 - 3d^9 4s$ (J = 2) transitions have therefore been observed as the strongest lines from the outer regions of the DITE plasma column. These lines are shown in the upper spectrum of figure 1 and their wavelengths are included in table 3.

$3d^n - 3d^{n-1}4s$ electric quadrupole transitions are also possible in Mo XIV, Mo XVI and higher ionization stages. However in these ions odd parity configurations, $3d^{10}4p$ in Mo XIV and $3p^5 3d^{n+1}$ in Mo XVI to Mo XXIV, lie between the $3d^{n-1}4s$ levels and the $3d^n$ levels of the ground configuration. Consequently all $3d^{n-1}4s$ levels in these ions, other than the Mo XVI J = 7/2, 9/2 levels and the Mo XVII J = 6 level, may also decay by electric dipole radiation to $3p^5 3d^{n+1}$ ($3d^{10}4p$ in Mo XIV) levels. On comparing observation with calculation the four strongest electric quadrupole transitions from the Mo XVI $3d^8 4s$ (J = 7/2, 9/2) levels have been clearly identified in the DITE spectrum. A fifth strong line at 54.33 Å is also tentatively identified in this way. The lines are shown in figure 1 and their wavelengths are given in table 4. Lines have also been observed close to the calculated positions of the two Mo XVII $3d^8$ (J = 4) - $3d^7 4s$ (J = 6) transitions but the observation is not sufficiently unambiguous to justify listing them in table 5.

Mo XVI $3p^5 3d^{10} - 3d^8 4s$ (J = 1/2, 3/2, 5/2) electric dipole transition probabilities have also been calculated. In general they are less than the calculated probabilities of electric quadrupole transitions from the $3d^8 4s$ upper levels so that in principle it is possible to observe many more 3d - 4s forbidden lines in Mo XVI and higher ionization stages. There is no clear evidence of the Mo XVI $3d^9 - 3d^8 4s$ (J = 1/2, 3/2, 5/2) lines in the DITE spectrum however. Their calculated electric quadrupole transition probabilities are all less than those of the four strongest $3d^9 - 3d^8 4s$ (J = 7/2, 9/2) observed lines. It should also be noted that only $3d^9 + 3d^8 4s$ configuration mixing has been included in the calculations. Inclusion of further mixing in the upper and lower configurations will probably increase the probability of electric dipole transitions and thus tend to quench electric quadrupole transitions from the J = 1/2, 3/2, 5/2 levels.

We thus summarize our findings for Mo XIII to XXIX as follows. It is possible to identify unambiguously the important transitions to the ground state in the lower degrees of ionization. 3d - 4s, 3d - 4p and 3d - 4f transitions in Mo XV and 3d - 4s 3d - 4p, 3d - 4f and 3p - 3d transitions in Mo XVI have all been identified and listed in detail (Tables 3 and 4). For Mo XVII and higher degrees of ionization a detailed analysis becomes rapidly more difficult. Nonetheless it has proved possible to analyse Mo XVII $3d^8$ - $3d^7 4p$ transitions in detail (Table 5) and work is in progress to achieve similar results for 3d - 4p transitions in Mo XVIII, Mo XIX and possibly Mo XX. The increasing tendency of lines to merge into diffuse bands of emission as the 3d-subshell becomes half full means that it may be difficult to achieve more than a general agreement between the calculated and observed band profiles in these ions although, as there is little overlap between different stages of ionization and transitions are mainly from the ground state, these bands should still be useful for diagnostic purposes. For 3p - 3d transitions in Mo XVI and higher degrees of ionization the main problem is the large overlap of lines from different degrees of ionization. A reasonable agreement between calculation and observation is possible for Mo XVII and higher stages of ionization but there are likely to be ambiguities due to line coincidences which will make their use for diagnostics difficult even if clearer identifications are possible from isoelectronic comparisons.

3d - 4f transitions tend to overlap 3d - 4p transitions in lower stages of ionization. In Mo XV and Mo XVI the two groups have been largely separated but it is clear from figure 8 that the Mo XX $3d^5$ - $3d^4 4p$ band is much stronger than would be expected if upper levels are populated purely by ground state excitation (figure 9). It will thus be difficult to separate 3d - 4f transitions in Mo XVII and higher degrees of ionization from 3d - 4p transitions in different stages of ionization.

From Mo XX to XXIX it is very hard to make detailed $\Delta n = 1$ assignments. There is considerable overlap between $\Delta n = 1$ transitions in many different ionization species and, as shown in figure 9, no transition can be disregarded completely for these ions. Moreover the high population of $3p^{n-1}3d^{m+1}$ levels in Mo XXI to Mo XXVIII will make it difficult to observe the simpler ground state transitions in Mo XXIV and XXV. Mo XXVI to XXIX will almost certainly radiate in the 30 to 16 Å region but the diffuseness of emission combined with the overlap problem will make it very difficult to

establish their presence in the plasma. The problems in identifying Mo XXX (Al-like) lines mentioned in section 5.2, namely the complexity resulting from the existence of three open subshells in excited configurations, are in fact further examples of the influence of inner subshell excitation, the 3s-subshell in this case. It is not until the n = 3 shell is almost empty, Mo XXXI (Mg-like) and Mo XXXII (Na-like), that the possibility of exciting an inner subshell of the same n as the valence subshell disappears and detailed analysis becomes practicable.

6. CONCLUSIONS

The general features of molybdenum emission likely to occur in Tokamaks at temperatures of less than 1.5 keV have been identified by comparison with ab initio calculations. Detailed analyses have been given for ion stages at the beginning and end of the n = 3 row of isoelectronic sequences, viz for Mo XXXII (Na-like), Mo XVI (Co-like), and, to a lesser extent, Mo XXXI (Mg-like) and Mo XVII (Fe-like). Altogether about one hundred new lines from very highly stripped ions (Mo XXX to Mo XXXII) are listed for the first time. For the lower ionization stages (Mo XV, Mo XVI, Mo XVII) about thirty-five new lines are listed and about fifty-five new identifications are given. It has been shown that for intermediate ionization stages (Mo XVIII to Mo XXIX) unambiguous detailed identifications will be mostly very hard to achieve due to the influence of inner subshell excitation. As a consequence it will be very difficult to derive absolute concentration estimates for these ions on the basis of observed emission. Earlier identifications for the Ni-like ion Mo XV have been confirmed and additionally, seven forbidden Mo XV and Mo XVI transitions which are strong features in the DITE Tokamak spectrum have been identified

The effects of inner subshell excitation, which have been discussed and illustrated here for molybdenum, are of quite general importance in the spectra of highly stripped heavy elements.

ACKNOWLEDGEMENTS

We wish to acknowledge our collaboration with the DITE group in this study and the invaluable assistance of A H Jones in operating the Nd laser.

REFERENCES

Aglitskii E.V., Boiko, V.A., Krokhin, O.N., Pikuz S.A. and Faenov A.Ya., 1975, Sov. J. Quant. Electron 4, 1152-1153.

Alexander E., Even-Zohar M., Fraenkel B.S. and Goldsmith S., 1971, JOSA 61, 508-514.

Cowan, R.D. and Griffin D.C., 1976, JOSA, 66, 1010-1014.

DITE Tokamak Group, 1977. Culham Laboratory Reports CLM-P492 and CLM-P502. To be published in Proc. of 8th Conference on Controlled Fusion and Plasma Physics, Prague 1977.

Édlen B., 1947, Physica, 13, 545-554.

Equipe TFR, 1975, Nuclear Fusion, 15, 1053-1066.

Froese-Fischer C., 1972, Computer Phys. Comm. 4, 107-116.

Hinnov E., Johnson L.C., Meservey E.B. and Dimock D.L., 1972, Plasma Phys. 14, 755-762.

Hinnov E., 1976, Phys. Rev. A., 14, 1533-1541.

Klapisch M., Perel R. and Weil D., 1976, CEA-Euratom report No. EUR-CEA-FC-827.

Peacock N.J., Galanti M., Jones, A.H. and Lawson K.D., 1977, to be published.

Schwob J.L., Klapisch M., Finkenthal M., Schweitzer N. and TFR group, 1977, Phys. Lett. 62A, 85-89.

Speer R.J., (1976), Space Science Instrumentation, 2, 463-487.

Table 1 Mo XXXII (Na-like) lines

Observed λ(Å) ± 0.005	I	Calculated λ	gf	transition	Calculated transitions too weak to be seen transition	λ	gf
10.197	2	10.21	.234	$3d_{3/2} - 6f_{5/2}$	$3d_{5/2} - 6f_{5/2}$	10.27	.017
10.241	3	10.26	.332	$3d_{5/2} - 6f_{3/2}$			
10.272	3	10.29	.116	$3s_{1/2} - 5p_{3/2}$			
10.323	2	10.33	.058	$3s_{1/2} - 4p_{1/2}$			
10.749	4	10.76	.240	$3p_{1/2} - 5d_{3/2}$	$3p_{3/2} - 5d_{3/2}$	11.02	.047
10.994	7	11.01	.423	$3p_{3/2} - 5d_{5/2}$			
11.875	5	11.89	.658	$3d_{3/2} - 5f_{5/2}$	$3d_{5/2} - 5f_{5/2}$	11.96	.047
11.931	6	11.95	.935	$3d_{5/2} - 5f_{7/2}$			
14.376	10	14.38	.410	$3s_{1/2} - 4p_{3/2}$			
14.560	6	14.56	.202	$3s_{1/2} - 4p_{1/2}$			
15.002	6	15.00	.888	$3p_{1/2} - 4d_{3/2}$			
15.460	10	15.45	1.55	$3p_{3/2} - 4d_{5/2}$			
15.509	2	15.50	.172	$3p_{3/2} - 4d_{3/2}$			
16.496	2	16.48	.112	$3p_{1/2} - 4s_{1/2}$			
17.047	7	17.04	3.83	$3d_{3/2} - 4f_{5/2}$			
17.099	2	17.09	.216	$3p_{3/2} - 4s_{1/2}$			
17.148	8	17.15	5.44	$3d_{5/2} - 4f_{7/2}$	$3d_{5/2} - 4f_{5/2}$	17.18	.271
18.591	3	18.59	.15	$3d_{5/2} - 4p_{3/2}$	$3d_{3/2} - 4p_{3/2}$	18.42	.018
					$3d_{3/2} - 4p_{1/2}$	18.72	.086
104.26	9	104.15	.362	$3p_{1/2} - 3d_{3/2}$			
126.94	9	126.18	.538	$3p_{3/2} - 3d_{5/2}$	$3p_{3/2} - 3d_{3/2}$	134.64	.056
127.81	10	127.61	.404	$3s_{1/2} - 3p_{3/2}$			
176.67	4	176.60	.146	$3s_{1/2} - 3p_{1/2}$			

Table 2 Spectra of highly ionized molybdenum other than Mo XXXII (Na-like) lines

Table 2.1 10-20 Å $\Delta n > 0$ transitions

Observed		Transition				Calculated		
λ(Å) ± 0.005	I	ion stage	config.	jj... - jj...	J - J	λ(Klapisch)	λ(present) gf	Likely transition of unidentified lines
10.50	1							XXXI 3s3d - 3s6f
10.53	2							
10.58	3							
10.63	2							
10.65	1							
11.00	band 4	XXXI	3s3p - 3s5d	1/2 1/2 - 1/2 3/2	0 - 1	11.032 §		
11.03								
11.101	2							
11.237	2							
11.26	band 2	XXXI	3s3p - 3s5d	1/2 3/2 - 1/2 5/2	2 - 2	11.275 §		
					2 - 3	11.282 §		
11.32				1/2 3/2 - 1/2 3/2	2 - 2	11.291 §		
					2 - 1	11.294 §		
11.338	1							
11.384	2							
11.430	1							
11.482	1	XXXI	3s3p - 3s5d	1/2 3/2 - 1/2 5/2	1 - 2	11.497		
12.212	1							
12.263	3							
12.330	5							
12.361	2							
12.40	band 2							
12.46								
12.48	band 1							
12.52								
12.55	band 1							XXXI 3s3d - 3s5f
12.60								
12.76	band 3							
12.83								
12.87	band 2							
12.97								

Table 2.1 (continued)

14.494	2								
14.577	1								
14.620	2								
14.665	1								
14.695	1								
14.743	5	XXXI	$3s^2$ - 3s4p	1/2 1/2 - 1/2 3/2	0 - 1	14.752	14.75	.423	
14.788	1								
14.809	1								
14.852	3	XXXI	$3p^2$ - 3p4d	1/2 1/2 - 3/2 5/2	0 - 1	14.842			
14.922	3	XXXI	$3s^2$ - 3s4p	1/2 1/2 - 1/2 3/2	0 - 1	14.929	14.94	.164	
		XXXI	$3p^2$ - 3p4d	1/2 1/2 - 3/2 3/2	0 - 1	14.927			
15.075	3								
15.134	2								
15.193	3	XXXI	3s3p - 3s4d	1/2 1/2 - 1/2 3/2	0 - 1	15.206			
		XXXI	$3p^2$ - 3p4d	1/2 3/2 - 3/2 5/2	2 - 1	15.195			XXXI
15.27	5	XXXI	3s3p - 3s4d	1/2 1/2 - 1/2 3/2	1 - 2	15.276*			3s3p - 3p4p
15.30 band	4	XXXI	3s3p - 3s4d	1/2 1/2 - 1/2 3/2	1 - 1	15.294*			
15.33	4								
also		XXXI	$3p^2$ - 3p4d	1/2 3/2 - 3/2 5/2	2 - 2	15.258§			
					3/2 5/2	2 - 3	15.273*		
					3/2 5/2	1 - 2	15.276*		
					3/2 3/2	1 - 0	15.268*		
					3/2 3/2	2 - 1	15.284§		
					3/2 3/2	1 - 1	15.302*		
					3/2 3/2	2 - 3	15.311§		
					3/2 3/2	2 - 2	15.340§		
15.411	2								
15.63	5								
15.64 band	5	XXXI	3s3p - 3s4d	1/2 3/2 - 1/2 5/2	2 - 2	15.639*			
					2 - 3	15.645*			
15.69	3	XXXI	3s3p - 3s4d	1/2 3/2 - 1/2 3/2	2 - 2	15.687*			
15.70	3				2 - 1	15.707*			
also		XXXI	$3p^2$ - 3p4d	3/2 3/2 - 3/2 5/2	2 - 1	15.643*			
					2 - 2	15.709*			
				3/2 3/2 - 3/2 3/2	2 - 3	15.765*			
15.77 band	6	XXXI	$3p^2$ - 3p4d		2 - 2	15.797§			
15.84	3			1/2 3/2 - 1/2 5/2	2 - 3	15.771*			
					2 - 2	15.776*			
					1 - 2	15.795§			

Table 2.1 (continued)

				1/2 3/2 - 1/2 3/2	2 - 1	15.809§		
					1 - 1	15.829§		
					2 - 2	15.830§		
					1 - 2	15.850§		
15.87 15.91	}band 1							
15.962	2							
16.003	2	XXXI	$3p^2$ - 3p4d	3/2 3/2 - 3/2 5/2	0 - 1	16.027		
16.046	4	XXXI	3s3p - 3s4d	1/2 3/2 - 1/2 5/2	1 - 2	16.068		
16.08 16.14	}band 3	XXXI	$3p^2$ - 3p4d	3/2 3/2 - 3/2 3/2	0 - 1	16.126§		
	also	XXXI	3s3p - 3s4d	1/2 3/2 - 1/2 3/2	1 - 2	16.119§		
					1 - 1	16.140§		
16.23 16.33	}band 1	XXXI	$3p^2$ - 3p4d	3/2 3/2 - 1/2 5/2	2 - 3	16.245§		
					2 - 2	16.259§		
				3/2 3/2 - 1/2 3/2	2 - 1	16.294§		
					2 - 2	16.317§		
16.754	3							
17.380	2	XXXI	3s3d - 3s4f	1/2 3/2 - 1/2 7/2	2 - 3	17.416	17.39	0.1
17.47 17.51	}band 4			1/2 3/2 - 1/2 5/2	1 - 2	17.480*	17.45	2.86§
				1/2 5/2 - 1/2 7/2	3 - 3	17.491§	17.48	0.006§
				1/2 3/2 - 1/2 5/2	2 - 3	17.526§	17.51	3.61*
					2 - 2	17.535§	17.51	0.462*
17.59	6			1/2 5/2 - 1/2 7/2	3 - 4	17.586*	17.58	6.08*
				1/2 5/2 - 1/2 5/2	3 - 3	17.602§	17.59	0.519*
17.677	1				3 - 2	17.611§	17.60	0.015§
17.84	2							
17.89	2			1/2 5/2 - 1/2 7/2	2 - 3	18.021§	17.89	3.38*
17.96 18.13	}band 4 2			1/2 5/2 - 1/2 5/2	2 - 3	18.139§	18.00	0.003§
17.982	2				2 - 2	18.148§	18.01	0.008§
18.16 18.24	}band 2							
18.452	2							
18.492	1							

"band" denotes an unresolved group of lines. In general the wavelengths of emission peaks within the bands are listed here.

* The calculated wavelength corresponds to an emission peak in the observed band.

§ The calculated transition does not correspond to an observed peak but may contribute to the overall strength of the band.

Table 2.2 85-140 Å $\Delta n = 0$ transitions

Observed		Transition				Calculated		
λ(Å) ± 0.02	I	ion stage	configuration	jjj.. - jj...	J - J	λ (Klapisch)	λ(present)	gf
87.44	2							
87.72	2							
89.05	1							
89.65	1							
89.98	2							
91.47	2							
91.66	1							
91.86	2							
92.53	4	XXX	$3s^2 3p - 3s^2 3d$	$(\frac{1}{2})^2$ 1/2 - $(\frac{1}{2})^2$ 3/2	1/2 - 3/2	92.682	93.51	0.606
94.71	4	XXXI	$3p^2 - 3p3d$	1/2 1/2 - 1/2 3/2	0 - 1	86.906	98.74	0.701
94.95	3	XXXI	3s3p - 3s3d	1/2 1/2 - 1/2 3/2	0 - 1	94.108	94.68	0.194
95.11	2							
95.44	2							
96.52	4	XXXI	3s3p - 3s3d	1/2 1/2 - 1/2 3/2	1 - 2	96.40	96.23	0.253
96.82	3	XXXI	$3p^2 - 3p3d$	1/2 3/2 - 3/2 3/2	2 - 3	96.479	98.37	0.54
97.93	4	XXXI	$3p^2 - 3p3d$	1/2 3/2 - 3/2 3/2	1 - 1	96.703	97.38	0.24
98.20	3	XXXI	3s3p - 3s3d	1/2 1/2 - 1/2 3/2	1 - 1	98.108	98.17	0.127
98.92	1							
100.39	3	XXXI	$3s3p - 3p^2$	1/2 1/2 - 3/2 3/2	1 - 2	100.260	99.37	0.318
100.58	7	XXX	$3s^2 3p - 3s^2 3d$	$(\frac{1}{2})^2$ 3/2 - $(\frac{1}{2})^2$ 5/2	3/2 - 5/2	101.938	106.03	1.07
101.05	3							
101.63	4	XXXI	$3p^2 - 3p3d$	1/2 3/2 - 3/2 3/2	1 - 2	101.789	101.83	0.33
101.97	3	XXXI	$3p^2 - 3p3d$	1/2 3/2 - 3/2 3/2	2 - 2	100.987	102.68	0.28
103.33	1	XXXI	$3p^2 - 3p3d$	3/2 3/2 - 3/2 5/2	2 - 3	101.44	104.11	0.15
103.56	1							
103.74	3							
103.94	3							
105.58	4	XXX	$3s^2 3p - 3s3p^2$	$(\frac{1}{2})^2$ 3/2 - $\frac{1}{2}(3/2)^2(2)$	3/2 - 3/2	103.359	108.21	0.853
106.91	2							
108.18	1							
108.32	4	XXXI	3s3d - 3p3d	1/2 5/2 - 3/2 5/2	3 - 3	108.607	108.30	0.144
108.66	3							
109.44	2							

Table 2.2 (continued)

112.65	5	XXXI	$3s3p - 3s3d_2$	$1/2\ 3/2 - 1/2\ 5/2$	2 - 3	112.362	112.08	0.680
112.95	3	XXX	$3s^23p - 3s3p^2_2$	$(\frac{1}{2})^2\ 1/2 - \frac{1}{2}\frac{1}{2}(1)3/2$	1/2 - 1/2	110.732	114.09	0.45
113.50	2	XXX	$3s^23p - 3s3p^2_2$	$(\frac{1}{2})^2\ 3/2 - \frac{1}{2}(3/2)^2(0)$	3/2 - 1/2	110.675	113.53	0.349
113.88	7	XXXI	$3s3p - 3s3d$	$1/2\ 3/2 - 1/2\ 5/2$	1 - 2	112.721	115.77	1.11
115.11	3	XXX	$3s^23p - 3s^23d$	$(\frac{1}{2})^2\ 3/2 - (\frac{1}{2})^2\ 3/2$	3/2 - 3/2	114.155	115.86	0.309
115.27	2	XXXI	$3s3p - 3s3d$	$1/2\ 3/2 - 1/2\ 3/2$	2 - 2	115.575	115.65	0.319
115.53	2	XXXI	$3p^2 - 3p3d$	$3/2\ 3/2 - 3/2\ 5/2$	2 - 2	114.763	116.39	0.26
115.97	10	XXXI	$3s^2 - 3s3p$	$1/2\ 1/2 - 1/2\ 3/2$	0 - 1	114.842	117.51	0.537
116.91	2	XXXI	$3p^2 - 3p3d$	$3/2\ 3/2 - 3/2\ 5/2$	0 - 1	115.633	118.76	0.37
117.66	1	XXXI	$3s3p - 3p^2$	$1/2\ 1/2 - 1/2\ 3/2$	0 - 1	117.010	117.27	0.215
117.90	3	XXXI	$3p^2 - 3p3d$	$3/2\ 3/2 - 3/2\ 3/2$	2 - 3	117.939	119.97	0.67
118.48	2	XXXI	$3p^2 - 3p3d$	$1/2\ 3/2 - 1/2\ 5/2$	1 - 2	118.869	118.85	0.36
118.74	1	XXXI	$3p^2 - 3p3d$	$3/2\ 3/2 - 3/2\ 3/2$	2 - 1	117.206	119.65	0.14
118.96	1	XXXI	$3p^2 - 3p3d$	$1/2\ 3/2 - 1/2\ 5/2$	2 - 2	117.778	120.00	0.15
120.86	2	XXXI	$3s3d - 3p3d$	$1/2\ 3/2 - 3/2\ 3/2$	1 - 1	120.290	121.43	0.257
121.07	3	XXXI	$3s3d - 3p3d$	$1/2\ 3/2 - 3/2\ 5/2$	2 - 2	120.276	121.01	0.58
121.30	3	XXXI	$3p^2 - 3p3d$	$1/2\ 3/2 - 1/2\ 5/2$	2 - 3	120.029	121.79	0.15
121.70	3	XXXI	$3s3d - 3p3d$	$1/2\ 3/2 - 3/2\ 3/2$	1 - 0	120.609	121.81	0.116
122.36	2	XXXI	$3s3p - 3p^2$	$3/2\ 3/2 - 3/2\ 3/2$	2 - 2	121.168	120.22	0.306
		XXXI	$3s3p - 3p^2$	$1/2\ 1/2 - 1/2\ 3/2$	1 - 2	123.638	121.47	0.196
		XXXI	$3s3p - 3p^2$	$1/2\ 1/2 - 1/2\ 3/2$	1 - 1	122.459	122.67	0.139
124.19	1	XXXI	$3s3p - 3p^2$	$1/2\ 3/2 - 3/2\ 3/2$	1 - 0	123.813	127.70	0.221
124.48	1	XXXI	$3s3d - 3p3d$	$1/2\ 3/2 - 3/2\ 3/2$	2 - 3	123.769	124.89	0.160
124.69	1	XXXI	$3s3d - 3p3d$	$1/2\ 5/2 - 3/2\ 5/2$	3 - 2	124.006	125.19	0.131
		XXXI	$3s3d - 3p3d$	$1/2\ 5/2 - 3/2\ 5/2$	2 - 1	127.336	126.05	0.381
		XXXI	$3s3d - 3p3d$	$1/2\ 5/2 - 3/2\ 3/2$	3 - 3	127.679	129.34	0.298
		XXXI	$3s3d - 3p3d$	$1/2\ 3/2 - 3/2\ 3/2$	1 - 2	128.246	128.44	0.182
133.10	6	XXXI	$3s3d - 3p3d$	$1/2\ 5/2 - 3/2\ 5/2$	2 - 3	132.801	129.99	1.48
136.06	3	XXXI	$3s3d - 3p3d$	$1/2\ 5/2 - 3/2\ 5/2$	3 - 4	135.779	135.46	0.874

Calculated wavelengths are listed only for transitions whose gf exceeds 0.1. This value has been chosen so that the number of calculated transitions approximately equals the number of observed lines. Agreement between observation and calculation is reasonably good for the five lines with $I \geq 5$. Otherwise detailed assignments should not be inferred from the comparison.

Table 3 Mo XV (Ni-like) lines

Comments	Observed λ(Å)	Observed ν(cm^{-1})	Calculated λ(Å)	Lower Level $3d^{10}\ ^1S$ J	Upper Level J′	Upper Level Designation
	$3d^{10}-3d^9 4s$					
DN	58.833	1699737	59.04	0	2	$(2\frac{1}{2},\frac{1}{2})$
DN	57.920	1726535	58.11	0	2	$(1\frac{1}{2},\frac{1}{2})$
	$3d^{10}-3d^9 4p$					
A	50.920	1964000	51.04	0	1	^3P
A	50.435	1982738	50.56	0	1	^1P
A	49.899	2004054	50.02	0	1	$(1\frac{1}{2},1\frac{1}{2})$
	$3d^{10}-3d^9 4f$					
SN	36.212	2761525	36.12	0	1	^3D
T	35.377	2826692	35.31	0	1	^1P

D Forbidden lines, observed in the Culham Tokamak, DITE.

A Lines first listed by Alexander et al. (1971). The 50.92 Å line was not seen in the present work (see text).

S Uncertain identification. This line lies in the Mo XIX $3d^6-3d^5 4p$ band.

N New lines.

T Line also reported in TFR Tokamak (Schwob et al. 1977).

Table 4 Mo XVI (Co-like) lines

Line Number (Figures 6 and 8)	Comments	Observed λ(Å) $\pm$ 0.01	ν(cm^{-1})	Calculated λ (Å)	Lower Level $3d^9\ ^2D$ J	Upper Level J′ Designation*
		$3d^9-3p^5 3d^{10}$				
	E	77.450	1291100	75.63	$1\frac{1}{2}$	$1\frac{1}{2}$ ^2P
	E	75.861	1318200	74.06	$2\frac{1}{2}$	$1\frac{1}{2}$ ^2P
	E	69.580	1437190	68.25	$1\frac{1}{2}$	$\frac{1}{2}$ ^2P
		$3d^9-3d^8 4s$				
	N	54.33	1840693	54.37	$1\frac{1}{2}$	$3\frac{1}{2}$ ($^3F_3, \frac{1}{2}$)
	N	54.07	1849374	54.18	$2\frac{1}{2}$	$3\frac{1}{2}$ ($^3F_4, \frac{1}{2}$)
	N	53.48	1870014	53.55	$2\frac{1}{2}$	$3\frac{1}{2}$ ($^3F_3, \frac{1}{2}$)
	N	52.68	1898254	52.78	$1\frac{1}{2}$	$3\frac{1}{2}$ ($^1G_4, \frac{1}{2}$)
	N	51.90	1926712	52.02	$2\frac{1}{2}$	$4\frac{1}{2}$ ($^1G_4, \frac{1}{2}$)

Table 4 Mo XVI lines (continued)

Line number (Figures 6 and 8	Comments	Observed λ(Å) ±0.01	ν(cm^{-1})	Calculated λ(Å)	Lower Level $3d^9\ ^2D$ J	Upper Level J′	Designation*
		$3d^9-3d^8 4p$					
1	N	47.858	2089501	47.96	1½	1½	$(^3F_{2,\frac{1}{2}})$
	A	47.273	2115380	47.34	2½	1½	$(^3F)4G$
2		47.180	2119533	(47.26	1½	2½	$(^3F_{4,1\frac{1}{2}})$
				(47.26	1½	1½	$(^3P)4P$
3	N	47.070	2124495	47.13	1½	2½	$(^3F_{3,1\frac{1}{2}})$
4		46.852	2134403	(46.92	2½	2½	$(^3F)^2D$
				(46.88	2½	3½	$(^3F_{4,1\frac{1}{2}})$
5	N	46.787	2137332	46.85	1½	1½	$(^3F)4F$
6		46.716	2140581	46.77	1½	2½	$(^1D_{2,1\frac{1}{2}})$
7	N	46.622	2144929	46.71	1½	1½	$(^3P_{1,\frac{1}{2}})$
8		46.577	2146980	46.64	2½	2½	$(^3F_{4,1\frac{1}{2}})$
9		46.486	2151188	46.55	1½	1½	$(^3F)^2D$
10		46.373	2156422	46.42	2½	3½	$(^3F_{2,1\frac{1}{2}})$
11		46.302	2159737	46.34	2½	2½	$(^3F)^2F$
12		46.232	2162999	46.29	1½	1½	$(^1D)^2P$
13		46.138	2167436	(46.16	1½	2½	$(^1G)^2F$
				(46.16	2½	2½	$(^1D_{2,1\frac{1}{2}})$
14		46.044	2171836	(46.11	2½	1½	$(^3P_{1,\frac{1}{2}})$
				(46.10	2½	3½	$(^1G_{4,\frac{1}{2}})$
15		45.955	2176029	46.02	1½	2½	$(^3P_{1,1\frac{1}{2}})$
16	N	45.876	2179785	(45.95	1½	½	$(^3P_{1,1\frac{1}{2}})$
				(45.92	1½	1½	$(^3P)^2D$
17		45.827	2182132	45.87	2½	3½	$(^3P)4D$
18		45.775	2184583	45.81	1½	2½	$(^1G)^2F$
19		45.680	2189159	45.70	2½	1½	$(^1D)^2P$
20		45.579	2193987	45.61	1½	½	$(^3P_{2,1\frac{1}{2}})$
21		45.504	219587	(45.57	2½	2½	$(^1G)^2F$
				(45.52	2½	1½	$(^3P_{o,1\frac{1}{2}})$
22	N	45.296	2207686	45.34	2½	1½	$(^3P)^2D$
23		45.036	2220446	45.10	2½	3½	$(^1G_{4,1\frac{1}{2}})$
24	NS	44.517	2246329	44.62	1½	½	$(^1S)^2P$
		$3d^9-3d^8 4f$					
44	T	32.998	3030487	(32.96	2½	1½	$(^1G)^2P$
				(32.94	1½	1½	$(^3F)^2D$
				(32.94	1½	2½	$(^3P)^2F$
45	N	32.927	3037021	32.84	2½	2½	$(^1G)^2D$
46	T	32.877	3041640	32.81	2½	3½	$(^3P)^2F$

Mo XVI Lines (continued)

Line number (figure 8)	Comments	Observed λ(Å)	Observed ν(cm^{-1})	Calculated λ(Å)	Lower Level $3d^9\ ^2D$ J	Upper Level J′	Upper Level Designation*
		$3d^9$-$3d^8 4f$(cont.)					
47	N	32.697	3058385	(32.64 (32.64	$2\frac{1}{2}$ $2\frac{1}{2}$	$2\frac{1}{2}$ $1\frac{1}{2}$	$(^3F)^2D$ $(^3P)^2F$
48	N	32.329	3093198	32.36	$1\frac{1}{2}$	$2\frac{1}{2}$	$(^1S)^2F$
49	N	32.029	3122171	32.12	$2\frac{1}{2}$	$3\frac{1}{2}$	$(^1S)^2F$

* Upper level designations are given for the major component in the most appropriate coupling scheme. Thus for $3d^8 4\ell$ configurations LS levels are written as $3d^8(^{2S_1}L_1)4\ell\ ^{2S+1}L$ and jj levels are written as $(3d^8(^{2S_1+1}L_1)J_1,\ 4\ell\ J_2)$

E First measured and identified by Edlén(1947).

N New lines.

A Line reported by Alexander et al. (1971) but not observed in present work.

T Lines reported in TFR Tokamak (Schwob et al. 1977).

S Possibly Mo XVII.

All other observed wavelengths agree well with those listed by Alexander et al. (1971).

Table 5 Mo (Fe-like) Lines

Line number (figure 7)	Comments	Observed λ(Å) ± 0.1	Observed ν(cm^{-1})	Calculated λ(Å)	Lower Level $3d^8$ J	Lower Level $3d^8$ Term	Upper Level J′	Upper Level Designation*
		$3d^8$-$3d^7 4p$						
25		43.12	2319109	(43.16	1	^3P	1	$(^4P_{2\frac{1}{2}},1\frac{1}{2})$
				(43.12	4	^3F	4	$(^4F_{4\frac{1}{2}},1\frac{1}{2})$
26		43.04	2323421	43.03	4	^3F	3	$(^4F)^3D$
27		42.95	2328289	42.99	4	^1G	5	$(^2H_{5\frac{1}{2}},1\frac{1}{2})$
28		42.90	2331002	42.90	4	^1G	4	$(^2H)^1G$
29		42.87	2332634	42.89	2	^3F	3	$(^2G_{3\frac{1}{2}},\frac{1}{2})$
30		42.72	2340824	42.74	4	^3F	4	$(^4F)^3F$
31		42.62	2346316	(42.64	2	^1D	2	$(^2P_{1\frac{1}{2}},1\frac{1}{2})$
				(42.62	2	^3P	1	$(^4P_{\frac{1}{2}},1\frac{1}{2})$
				(42.62	2	^3P	3	$(^2D_{2\frac{1}{2}},1\frac{1}{2})$
32		42.56	2349624	(42.57	2	^3F	3	$(^2G_{4\frac{1}{2}},1\frac{1}{2})$
				(42.56	2	^1D	1	$(^2P_{\frac{1}{2}},1\frac{1}{2})$
33		42.49	2353495	(42.52	4	^1G	5	$(^2H_{4\frac{1}{2}},1\frac{1}{2})$
				(42.46	4	^3F	5	$(^2H_{5\frac{1}{2}},\frac{1}{2})$
34		42.41	2357934	42.43	3	^3F	4	$(^2H)^3G$
35		42.30	2364066	(42.30	2	^1D	1	$(^2F)^3D$
				(42.29	2	^1D	3	$(^2F_{1\frac{1}{2}},2\frac{1}{2})$
36		42.26	2366304	(42.27	2	^3F	2	$(^2G)^3F$
				(42.27	3	^3F	3	$(^2G_{3\frac{1}{2}},1\frac{1}{2})$
37		42.21	2369107	(42.22	4	^1G	3	$(^2D_{1\frac{1}{2}},1\frac{1}{2})$
				(42.21	3	^3F	2	$(^2G)^3F$
38	B	42.08	2376000	(42.15	2	^3P	3	$(^2H)^3G$
		to	to	(42.13	1	^3P	1	$(^2F)^3D$
		42.14	2373000	(42.13	4	^3F	3	$(^2P)^3D$
				(42.10	4	^3F	4	$(^2G_{4\frac{1}{2}},1\frac{1}{2})$
				(42.09	2	^1D	2	$(^2F_{3\frac{1}{2}},1\frac{1}{2})$
39		41.92	2385496	41.93	4	^3F	3	$(^4P_{2\frac{1}{2}},1\frac{1}{2})$
40		41.86	2388915	41.86	4	^1G	3	$(^2F)^1F$
41		41.80	2392344	(41.82	2	^3F	1	$(^2_3D)^1P$
				(41.81	4	^3F	4	$(^2G_{3\frac{1}{2}},1\frac{1}{2})$
				(41.81	2	^3P	2	$(^2F_{2\frac{1}{2}},1\frac{1}{2})$
				(41.55	4	^3F	4	$(^2_3D)^3F$
42		41.59	2404424	(41.54	4	^1G	3	$(^2_1D_{2\frac{1}{2}},\frac{1}{2})$
				(41.54	4	^3F	5	$(^2_1H_{5\frac{1}{2}},1\frac{1}{2})$
43		41.06	2435460	41.07	4	^1G	3	$(^2_1D_{1\frac{1}{2}},1\frac{1}{2})$

* Upper levels designations are given for the major components in the most appropriate coupling scheme. LS and jj notations as for Mo XVI $3d^8 4\ell$ configurations.

All lines listed here are newly observed.

B Band of lines.

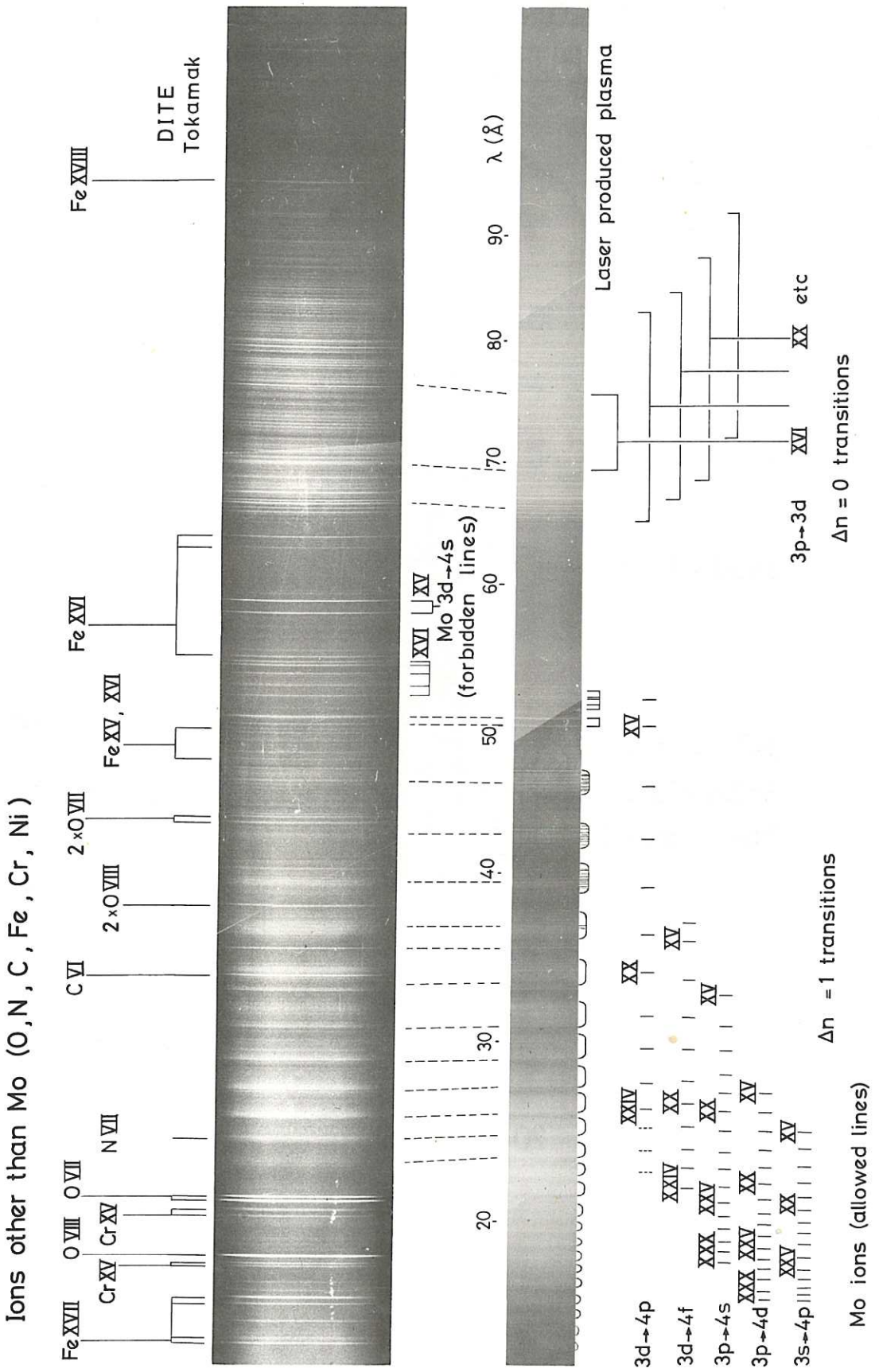

Fig.1 Comparison of molybdenum spectra between 10 and 100 Å observed in the Tokamak DITE (upper spectrum) and the laser-produced plasma at low beam intensities (lower spectrum).

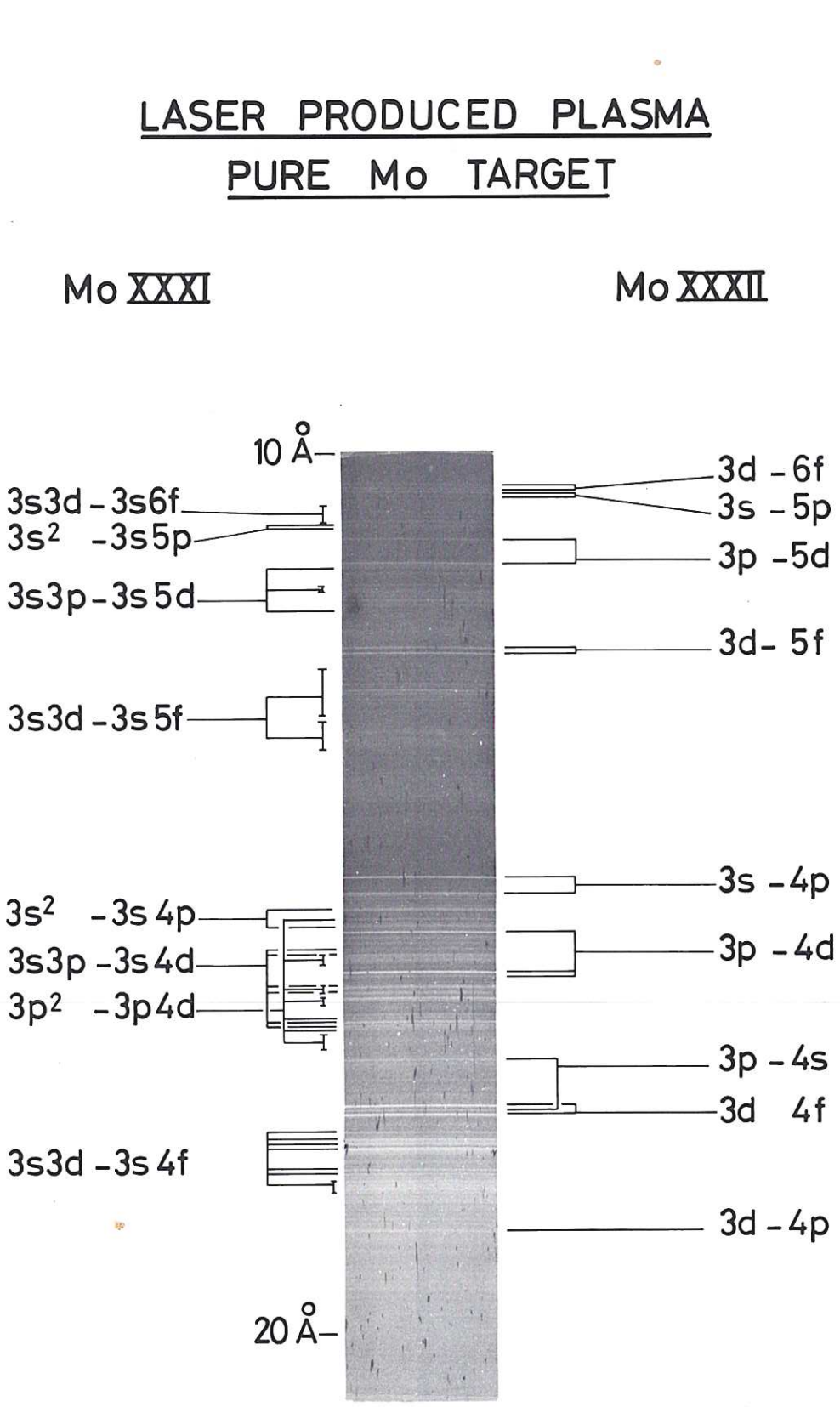

Fig.2 The spectrum of highly ionized molybdenum between 10 and 20 Å at high laser beam intensity.

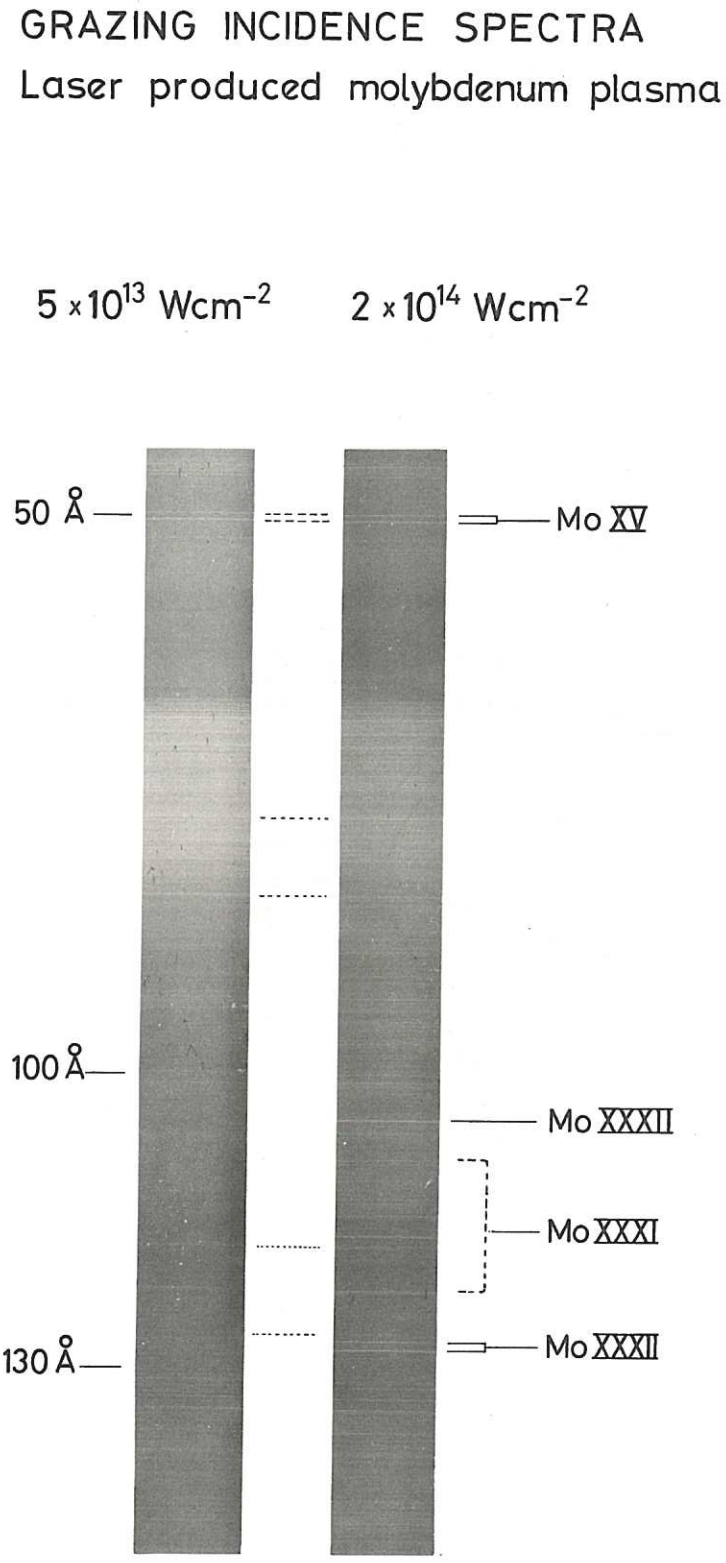

Fig.3 Comparison of molybdenum spectra between 50 and 140 Å at high and low laser beam intensities.

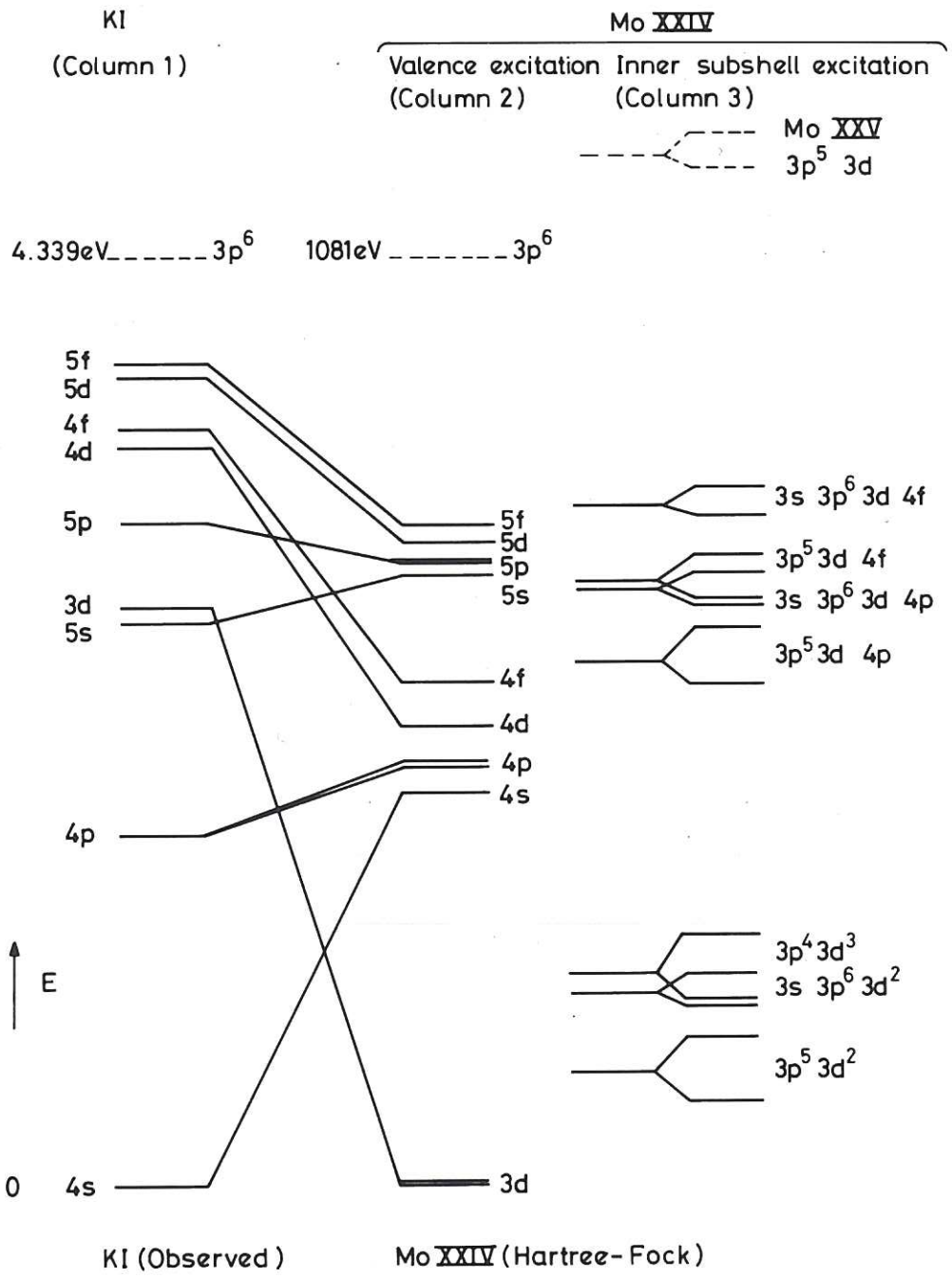

Fig.4 Comparison of observed K I energy levels with the energy levels of the K-like ion Mo XXIV. The Mo XXIV energies have been derived from Hartree-Fock calculations.

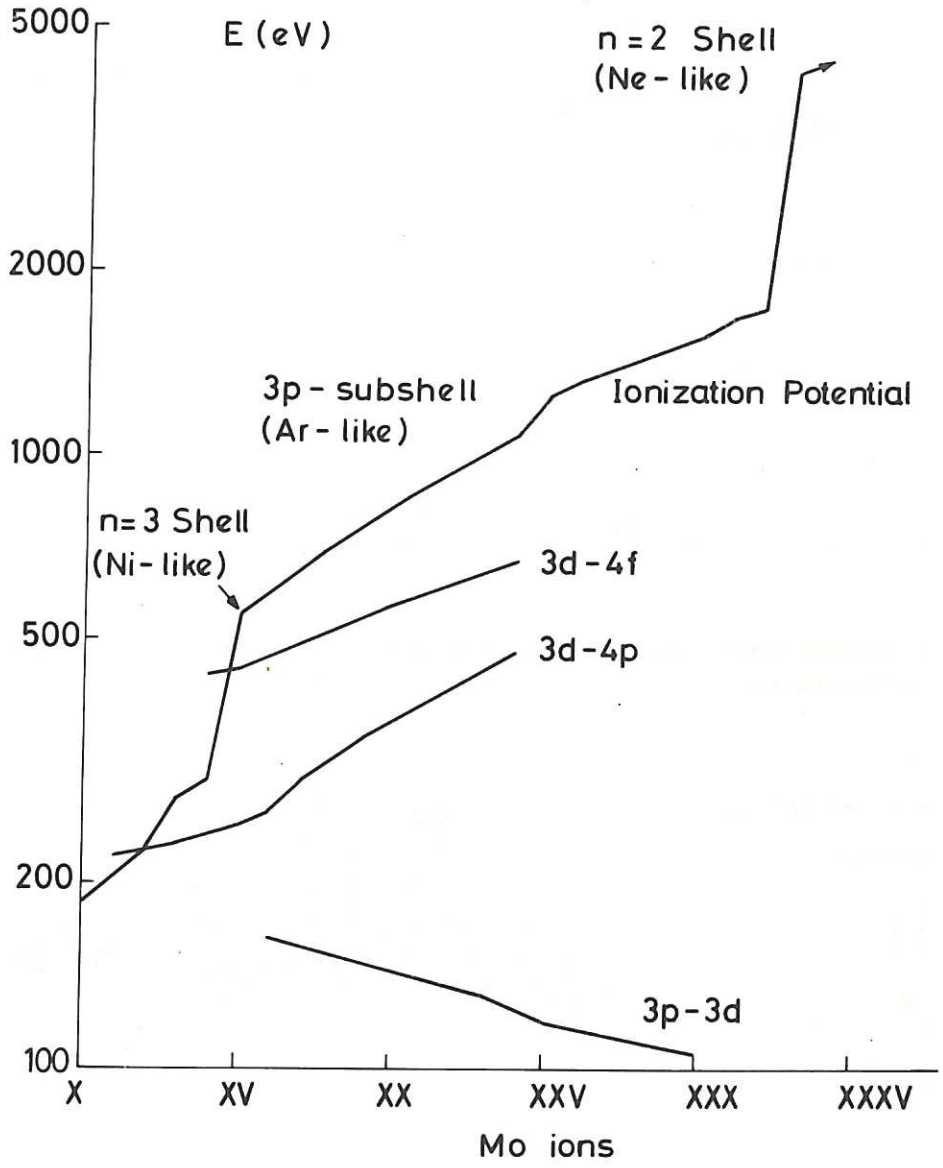

Fig.5 Variation of ionization potential and 3p–3d, 3d–4p and 3d–4f transition energies with ionization stage (from Mo X to Mo XXXIV). All energies are configuration average energies derived from Hartree-Fock calculations.

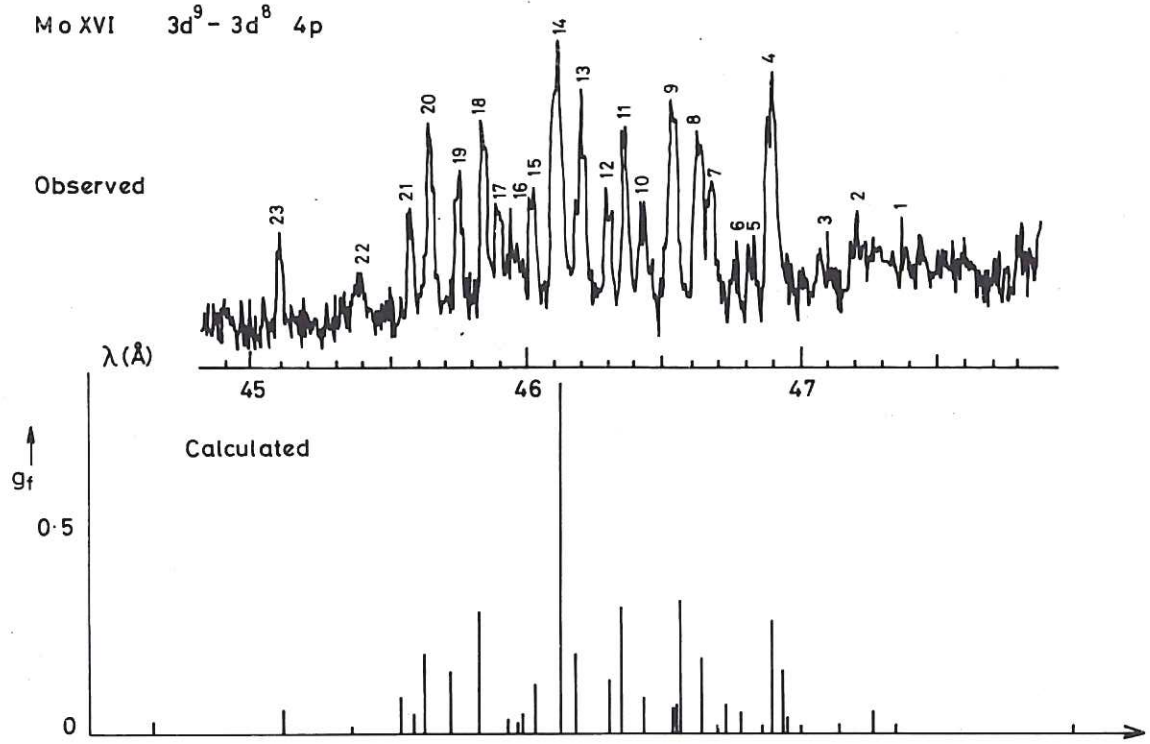

Fig.6 Comparison between microdensitometer trace of observed spectrum and calculation for Mo XVI $3d^9 - 3d^8 4p$ transitions.

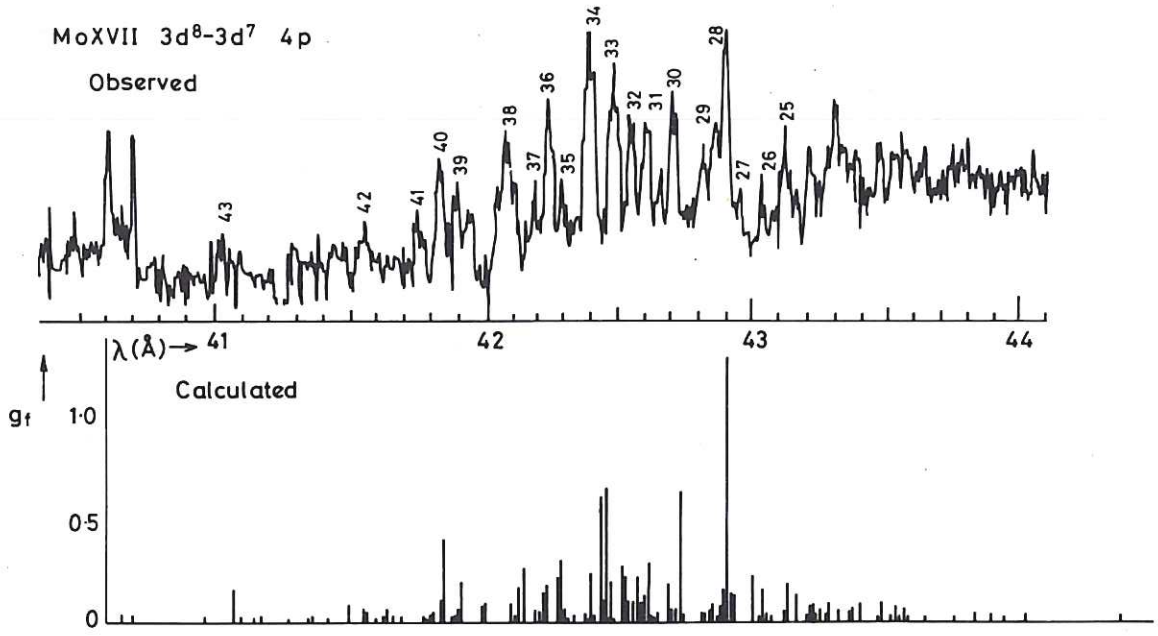

Fig.7 Comparison between microdensitometer trace of observed spectrum and calculation for Mo XVII $3d^8 - 3d^7 4p$ transitions.

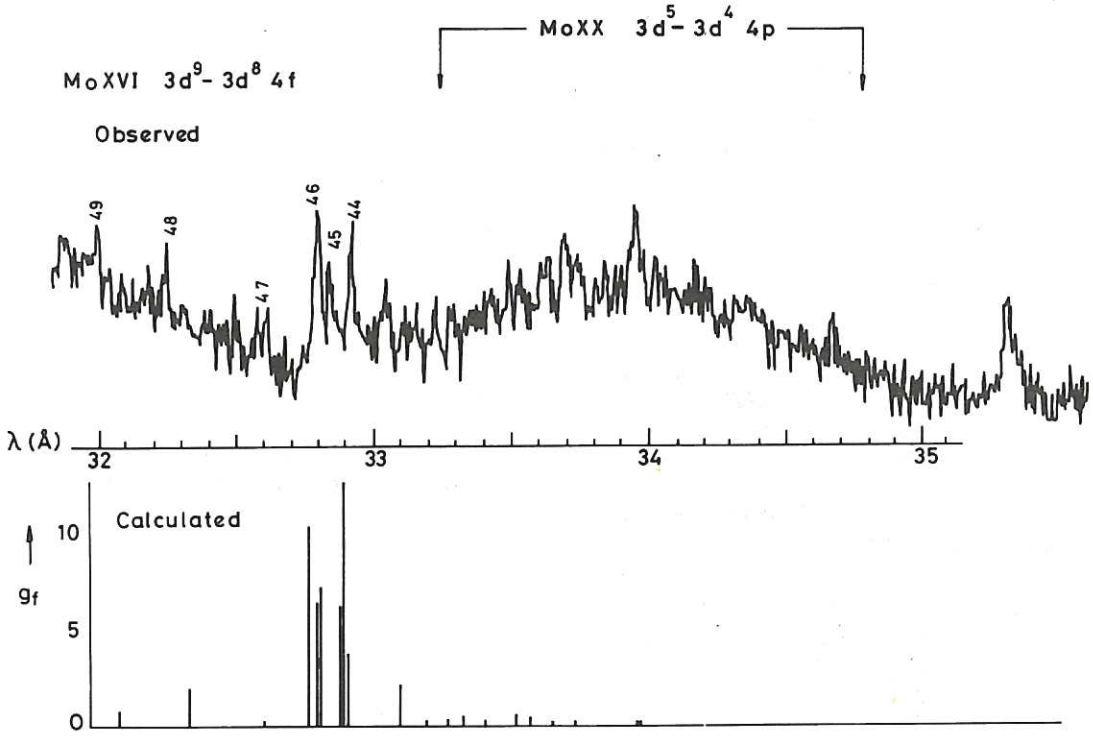

Fig.8 Comparison between microdensitometer trace of observed spectrum and calculation for Mo XVI $3d^9 - 3d^8 4f$ transitions.

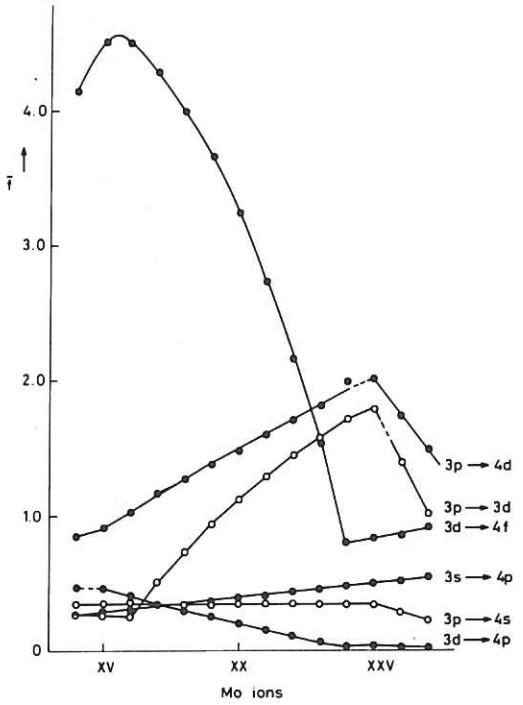

Fig.9 Variation with ionization stage of calculated mean array oscillator strength of $\Delta n = 0,1$ transitions ($\overline{f}$ was computed by summing f_{ij} over j levels of the upper configuration, and averaging over states of the lower configuration).

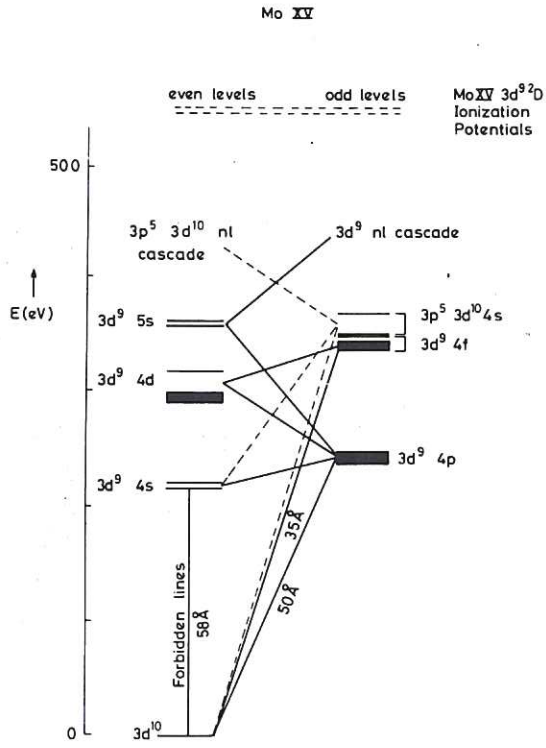

Fig.10 Mo XV energy level diagram. Energies are derived from Hartree-Fock calculations.

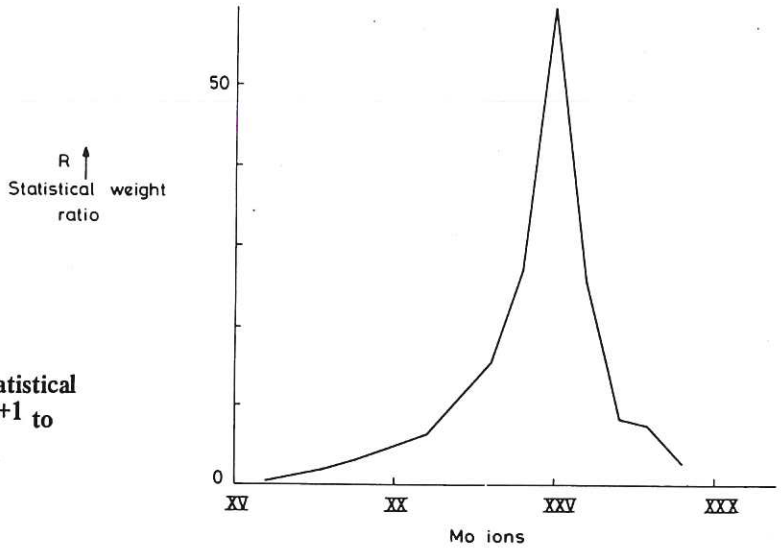

Fig.11 Variation of R, the ratio of the total statistical weight of the excited configuration $3p^{n-1}\,3d^{m+1}$ to that of the ground configuration $3p^{n}3d^{m}$ with ionization stage, (Mo XVI to Mo XXIX).